Live Cell Multiphoton Microscopy of Atherosclerotic Plaques in Mouse Aortas

7

Sara McArdle, Ekaterina Koltsova, Grzegorz Chodaczek, and Klaus Ley

Contents

7.1 Introduction . . . 156
7.1.1 Atherosclerosis . . . 156
7.1.2 Live Cell Microscopy . . . 157
7.1.3 Choice of Multiphoton Microscopy for Studying Atherosclerosis. . . . 159
7.2 Materials and Methods . . . 159
7.2.1 Aorta Harvest . . . 159
7.2.2 T Cell Harvest. . . . 160
7.2.3 Tissue Maintenance During Imaging . . . 162
7.2.4 Microscopy and Hardware . . . 163
7.2.5 Image Processing . . . 166
7.3 Results . . . 166
7.4 Conclusion and Future Work. . . . 168
References . . . 168

Abstract

Atherosclerosis is a chronic inflammatory disease with both innate and adaptive immune components. Various static methods have been applied to investigate mechanisms of atherosclerosis development. However, they did not allow for monitoring dynamic changes in leukocyte behavior in normal and atherosclerotic

S. McArdle
Division of Inflammation Biology, La Jolla Institute for Allergy and Immunology, 9420 Athena Circle, La Jolla, CA 92037, USA

Department of Bioengineering, University of California, San Diego, La Jolla, CA, USA

E. Koltsova • G. Chodaczek • K. Ley, MD (✉)
Division of Inflammation Biology, La Jolla Institute for Allergy and Immunology, 9420 Athena Circle, La Jolla, CA 92037, USA
e-mail: Klaus@liai.org

E. Aikawa (ed.), *Cardiovascular Imaging: Arterial and Aortic Valve Inflammation and Calcification*, DOI 10.1007/978-3-319-09268-3_7

aortas. Live cell imaging is necessary to study dynamic or transient leukocyte functions relevant to disease pathology, such as antigen presentation, cell migration, and cell-cell interaction. We developed a protocol for ex vivo multiphoton microscopy of atherosclerotic aortas and used it to demonstrate that antigen presentation may occur within the arterial wall. Aortas are harvested from transgenic reporter mice with fluorescent myeloid cells and then incubated with labeled T cells. The cells are imaged with a multiphoton microscope, while a superfusion system maintains the explant in physiologic condition. Cells are tracked from the videos, and their motion is quantified. This system was used to demonstrate antigen presentation in the arterial wall in the context of atherosclerosis.

7.1 Introduction

7.1.1 Atherosclerosis

Atherosclerosis is an underlying cause of most heart attacks, strokes, and other forms of cardiovascular disease, which is one of the leading causes of death worldwide [1]. It is a chronic inflammatory disease, characterized by plaque buildup in large and medium arteries. Within plaques, leukocytes actively mediate both pro- and anti-inflammatory processes [2]. Disease progression and plaque content have traditionally been studied using static end-point methods, including histology, immunohistochemistry, immunofluorescence, and flow cytometry of aortas [3]. These methods provide qualitative and quantitative data on the numbers and phenotypes of cells in the plaque, but cannot evaluate dynamic cell functions, such as cell motion and cell-cell interaction. Live cell imaging is necessary to study these transient processes to better understand their contribution to disease progression.

One dynamic cell function that is integral to inflammation is antigen presentation. This is a process by which an antigen-presenting cell takes up antigen from its microenvironment and processes it to be recognizable by T cells in the context of MHC molecules. When a T cell receptor (TCR) recognizes an antigenic peptide on MHC on the surface of an antigen-presenting cell (APC) and coactivator signals are present, the T cell becomes activated, proliferates, and produces cytokines that influence plaque development [4]. During the typical immune response, dendritic cells, a type of APC, take up antigen from the area of inflammation and migrate to local lymph nodes, where they present this antigen to naïve T cells, leading to the T cells' initial activation. These antigen-experienced T cells acquire new homing properties (adhesion molecules and chemokine receptors), enabling them to traffic back to the original site of insult, and they polarize to characteristic functional subsets. Interactions between APCs and T cells have been observed in nonlymphoid tissues [5], and recent in vitro data suggests that antigen presentation to antigen-experienced T cells occurs in the arterial wall [6, 7]. Unlike static methods, live cell imaging can uniquely take advantage of changes in T cell behavior (slowing down) while interacting with an APC [8, 9]

to demonstrate antigen presentation in the cells' native microenvironment. Here, we describe a technique to visualize leukocyte activity in the wall of healthy and atherosclerotic aorta explants using multiphoton microscopy [10].

7.1.2 Live Cell Microscopy

The choice of microscopy technique for imaging live cells in vivo or ex vivo depends on the optical properties of the target tissue and the spatial and temporal resolution needed to observe the phenomena in question. The four most common microscopy techniques for imaging ex vivo or in vivo are epifluorescence, spinning disk confocal, laser scanning confocal, and multiphoton [11, 12]. Each of these techniques has unique advantages and disadvantages for live cell fluorescence imaging (Table 7.1) [13, 14].

7.1.2.1 Epifluorescence Microscopy

Epifluorescence, or widefield, microscopy is frequently used for live imaging because of its high frame rate (up to 50 frames/s for a 512×512 pixel frame, depending on the camera [15]). Another advantage is that this technique can acquire transmitted light images, allowing for visualizing of tissue structure in combination with fluorescence. Unlike a confocal, all light that reaches the objective is collected, and therefore excitation intensity can be lowered to reduce photobleaching and phototoxicity. However, this leads to diminished lateral resolution due to out-of-focus light in thick tissues and explants. Epifluorescence microscopes cannot distinguish depth except via

Table 7.1 Advantages and disadvantages of common live cell imaging modalities

Method	Advantages	Disadvantages
Epifluorescence	Fast	Poor axial and lateral resolution
	Lower photobleaching than confocal	Limited to thin tissues Limited control of excitation wavelength
Spinning disk confocal (SDCM)	Fast	Low excitation tissue penetration
	Good axial and lateral resolution Less photobleaching than LSCM	Lower intensity and contrast than LSCM
Laser scanning confocal (LSCM)	Best resolution and contrast in XYZ	Slow Low excitation tissue penetration High photobleaching
Multiphoton	Deep tissue penetration	Slow
	Low photobleaching of out-of-focus planes	Poor axial resolution compared to LSCM and SDCM
	Good lateral resolution Single laser can excite broad range simultaneously	Difficult to sequentially excite different fluorophores

post-acquisition deconvolution [16] and so are inadequate for situations in which axial resolution is important. Epifluorescence microscopes use broad-spectrum lamps and control excitation wavelength through filter cubes. Filter wheels allow for rapid switching of excitation wavelength; however, different fluorophores must be analyzed sequentially, which decreases frame rate and may lead to poor registration between different colors in rapidly moving cells. Therefore, this technique is typically only used for samples with one or two fluorophores and only for thin tissues (<100 μm).

7.1.2.2 Confocal Microscopy

Confocal microscopy provides the best spatial resolution of the standard live cell techniques and so is often chosen for applications requiring resolution of subcellular structures. Spinning disk confocal systems can image at very high speeds (theoretically up to 2,000 fps [17], in practice highly limited by the CCD camera), making them ideal for imaging fast processes. If a very high speed is not necessary, laser scanning confocal systems can provide higher lateral and axial resolution with less noise (especially in weakly fluorescent samples), while still scanning up to 40 fps, depending on the image size. However, laser scanning confocal systems typically spend more time exciting each pixel, resulting in higher photobleaching and phototoxicity. Both types of confocal systems are limited by a small penetration depth (two to three times smaller than the maximum of a multiphoton microscope [18]) due to high scattering of visible excitation light by the sample. Unlike epifluorescence systems which use similar excitation wavelength, confocal microscopes retain high resolution in thick tissues by optically slicing with the confocal aperture. However, the aperture blocks a portion of the emitted light that reaches the detector, requiring more intense excitation and causing additional photobleaching than epifluorescence or multiphoton microscopy. The use of lasers of defined wavelengths makes it technically easier to image multiple fluorophores simultaneously, improving time resolution compared to epifluorescence microscopy. Typical imaging depths achieved by confocal microscopy are 100–200 μm.

7.1.2.3 Multiphoton Microscopy

Multiphoton microscopes excite the sample with a high-intensity, pulsed femtosecond laser with a long (infrared) wavelength to penetrate deeper into tissue with less scattering than confocal or epifluorescence microscopes (up to 500 μm) [19]. Thanks to the two-photon excitation, which only takes place in the objective's focal point, true optical slicing is achieved so only a small volume is excited at one time, minimizing the time each point in the sample is exposed to light while retaining good spatial resolution. Because there is no need for a confocal aperture, all of the emitted light that reaches the objective is collected, thus reducing the needed intensity of the excitation. Together, these phenomena reduce photobleaching and improve the signal intensity in thick tissues, making it a common choice for in vivo imaging. Most fluorophores have a broader two-photon excitation range than single-photon excitation [20], enabling the excitation of multiple fluorophores simultaneously. A disadvantage of this is that distinguishing fluorochromes by changing excitation wavelength is generally not feasible. Multiphoton microscopy has lower

resolution in all three axes than laser scanning confocal, dictated by the long excitation wavelength (typically 800–1,000 nm). The use of low-noise, high-dynamic-range photomultipliers improves sensitivity but drastically reduces acquisition speed compared to spinning disk confocal and epifluorescence microscopy. Better acquisition speeds can be realized by using a resonant scanner.

7.1.3 Choice of Multiphoton Microscopy for Studying Atherosclerosis

Atherosclerotic plaques in mouse aortas can be more than 100 μm thick [21], making two-photon excitation necessary for viewing the depth of the plaque. A low frame rate is sufficient for visualizing leukocyte movement within the arterial wall, because migration speeds are less than 1 μm/s. The low photobleaching inherent in multiphoton microscopy enables acquisition of long (~1 h) movies, which is necessary for quantifying slow migration. Multiphoton microscopy also uniquely enables the visualization of unlabeled collagen in the wall through second-harmonic generation [22]. We used multiphoton microscopy to visualize antigen presentation in the context of atherosclerosis [10].

7.2 Materials and Methods

7.2.1 Aorta Harvest

7.2.1.1 Background

Aortas can be obtained from healthy or atherosclerotic mice that have transgenically labeled leukocytes. Mice deficient in apolipoprotein E (*Apoe*$^{-/-}$), a protein involved in lipoprotein transport, are a common model for atherosclerosis. They rapidly develop plaques when fed a high-fat western diet (WD) [23]. To study the interaction between antigen-presenting myeloid cells and T cells in atherosclerotic plaques, we used *CD11c*^{YFP} mice, which express yellow fluorescent protein under the CD11c promoter [24]. This mouse has CD11b+ CD11c+ macrophages and dendritic cells in the plaque bright enough to be visualized with multiphoton microscopy. The precise relationship between YFP brightness and cell phenotype, including CD11c expression, needs to be established in each tissue and experimental setting. Non-atherosclerotic mice can be injected with 30 μg of CpG class B oligonucleotides (ODN 1826, Integrated DNA technologies), 2–3 h before sacrifice to induce myeloid cell recruitment to the aorta wall. Within atherosclerotic plaques, myeloid cells phagocytose lipids, scavenge dead cells, and secrete both pro- and anti-inflammatory cytokines [2].

7.2.1.2 Method

The mouse was killed by CO_2, and 0.5–1 mL of blood was withdrawn via cardiac puncture with a 25 G needle. The internal organs were removed, and then 10 mL of PBS (containing 20 U/mL heparin) were perfused through the aorta through the

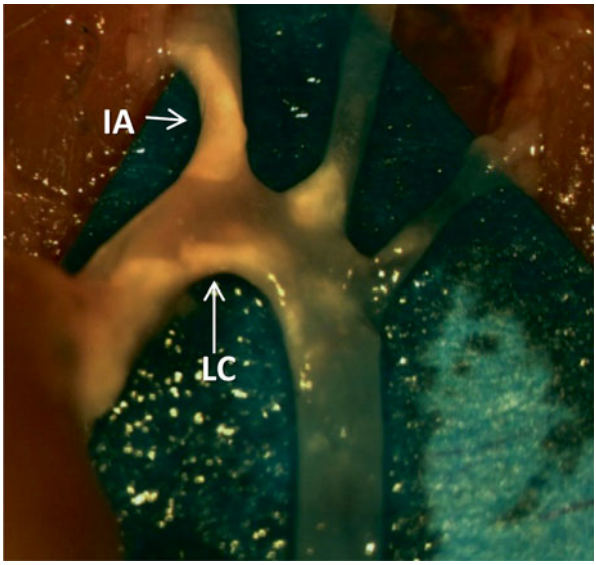

Fig. 7.1 The aorta of an *Apoe*$^{-/-}$ mouse that was fed WD for 12 weeks. After sacrifice, the aorta was perfused with PBS with 20 U/mL heparin and the artery was cleaned of fat (see Sect. 7.2.1.2) to reveal visible atherosclerotic plaque (opaque beige, *white arrows*). *IA* innominate artery, *LC* lesser curvature

heart. Using forceps and spring scissors, the fat and para-aortic lymph nodes were removed from around the artery. To maintain cell viability, it is important to disturb the wall of the aorta as little as possible, especially near the area that will be imaged, and to keep the tissue moist with PBS. The aorta was harvested, from its origin from the heart to above the renal arteries, including the branches to the innominate, left common carotid, and left subclavian arteries. Solid plaques develop first at the branch of the innominate artery from the aorta and also in the lesser curvature of the aorta. Both areas are suitable for imaging (Figs. 7.1 and 7.2). The artery was incubated overnight with T cells at 37 °C with 5 % CO_2 in complete RPMI 1640 media containing 10 % FBS, 1 % pen/strep, 2 mM L-Glu, 1 % NEAA, 1 mM HEPES, and 1 mM sodium pyruvate before imaging.

7.2.2 T Cell Harvest

7.2.2.1 Background

Theoretically, every T cell in a mouse may express a unique TCR that is specific for a different peptide. To investigate antigen-specific T cell activation, we used transgenic mice in which majority of CD4 T cells have a restricted TCR specificity to well-defined exogenous antigenic peptides. These mice are useful tools for studying antigen presentation because the presence of antigen can be easily controlled. We employed two different strains of mice with transgenic TCRs: OT-II, which have T cells specific for a peptide derived from ovalbumin [25], and SMARTA, which have T cells specific for a peptide derived from lymphocytic choriomeningitis virus (LCMV) [26] (see Table 7.2). Having two distinct TCR transgenic mice allowed us to image T cells with and without their cognate antigen in the same experimental setup to more accurately assess the specificity of antigen presentation in the aorta. Since neither antigen is present in a mouse, almost all T cells harvested from the

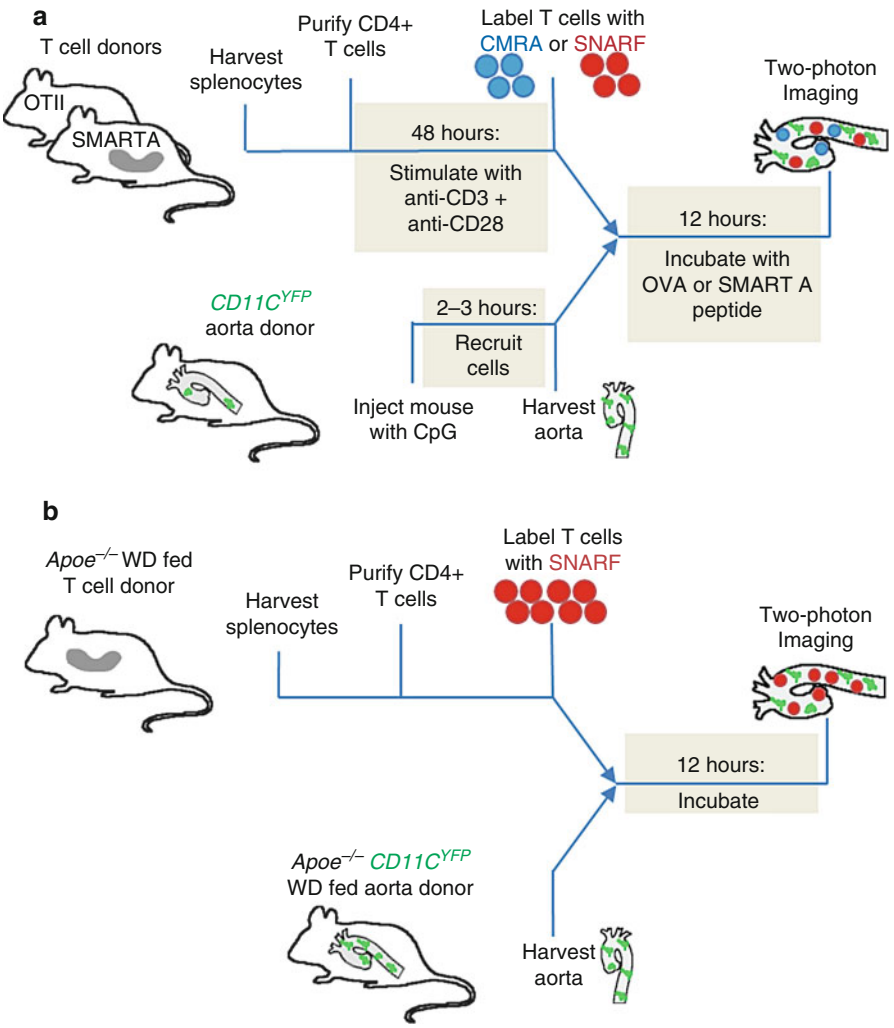

Fig. 7.2 Schematic timeline of procedure for imaging myeloid cells presenting antigen to T cells in the aorta wall. (**a**) To image antigen presentation with a known, exogenous antigen, CD4+ T cells with transgenic TCRs are harvested and purified from the spleen and restimulated in vitro. YFP+ myeloid cells are recruited to the aorta with an injection of CpG, and after 2–3 h the aorta is harvested. The T cells are labeled and incubated with the aorta in the presence of exogenously added antigenic peptide, and then the tissue is imaged using two-photon microscopy. (**b**) To image antigen presentation in the context of atherosclerosis, the aorta of an atherosclerotic mouse with YFP+ myeloid cells is harvested. CD4+ T cells are harvested and purified from an atherosclerotic mouse. The T cells are labeled and incubated with the aorta, and then the tissue is imaged using two-photon microscopy

transgenic mice are naïve. Naïve cells must be activated in vitro with anti-CD3 and anti-CD28 to maintain cell viability. To assay antigen presentation in the context of atherosclerosis, we also used polyclonal T cells from WD-fed *Apoe*$^{-/-}$ mice. The specific peptide that these cells recognize is unknown, but it is likely to be

Table 7.2 Sources of T cells and the peptides they recognize

Mouse strain	Antigen protein	Peptide recognized by TCR
OT-II	Ovalbumin	ISQAVHAAHAEINEAGR
SMARTA	Glycoprotein P13 from LCMV	GLNGPDIYKGVYQFKSVEFD
Apoe$^{-/-}$	Unknown endogenous, possibly ApoB100, HSP60, or oxLDL	Unknown

endogenously found in the aortas of atherosclerotic mice (see Table 7.2) [27–29]. Many T cells isolated from WD-fed atherosclerotic mice are endogenously activated, and so these cells do not require additional stimulation in vitro.

7.2.2.2 Method

$CD4^+$ T cells were harvested from the spleens of atherosclerotic or TCR transgenic mice using a Robosep-negative selection kit (Stem Cell Technologies). These cells were stimulated for 48 h with 8 μg/mL anti-CD3 and 8 μg/mL anti-CD28 (eBioscience) in complete RPMI 1640 media containing 10 % FBS, 1 % pen/strep, 2 mM L-Glu, 1 % NEAA, 1 mM HEPES, and 1 mM sodium pyruvate. T cells isolated from WD-fed atherosclerotic mice were not restimulated in vitro. The cells were differentially labeled with 2.5 μM SNARF (red fluorescent carboxylic acid, acetate, succinimidyl ester, Molecular Probes) or 3 μM CMRA (CellTracker Orange, Molecular Probes) for 10 min at 37 °C. 0.5 million labeled cells were incubated with the explanted aorta in 750 μL media overnight. T cells from atherosclerotic mice were incubated with an aorta from an atherosclerotic mouse, while T cells from mice with transgenic TCRs were incubated with a healthy aorta with or without 1 μM OVA peptide or SMARTA peptide (Table 7.2).

7.2.3 Tissue Maintenance During Imaging

To visualize realistic cell motion, it is necessary to keep the tissue under physiological temperature, pH, oxygen tension, and osmolarity throughout imaging. Immediately before imaging, we secure the aorta to a coverslip by gluing the ends of the tissue with Histoacryl glue (TissueSeal LLC) or Vetbond (3 M). Tissue that touches the glue is unsuitable for imaging, so only the ends of the aorta should be glued down and only the middle used for imaging. A system (Fig. 7.3) was built to keep the tissue warm and superfused with recirculating, oxygenated media throughout the imaging procedure. A reservoir of oxygenated media was created by bubbling gas (95 % oxygen, 5 % CO_2) through ~25 mL of complete RPMI 1640 without phenol red, with 2 mM L-glutamine, 1 % pen/strep, and 1 % FBS, in a 50 mL conical tube. The sample glued to the coverslip was placed in a 60 mm dish with the same solution. A peristaltic pump (Harvard Apparatus, MPII) circulated media at approximately 10 mL/min from the reservoir through an in-line solution heater (Warner Instruments, SF-28) to the dish. The dish was heated by a warmer (Warner Instruments, QE-2 Quick Exchange Platform), and both this and the in-line heater were controlled by a dual feedback

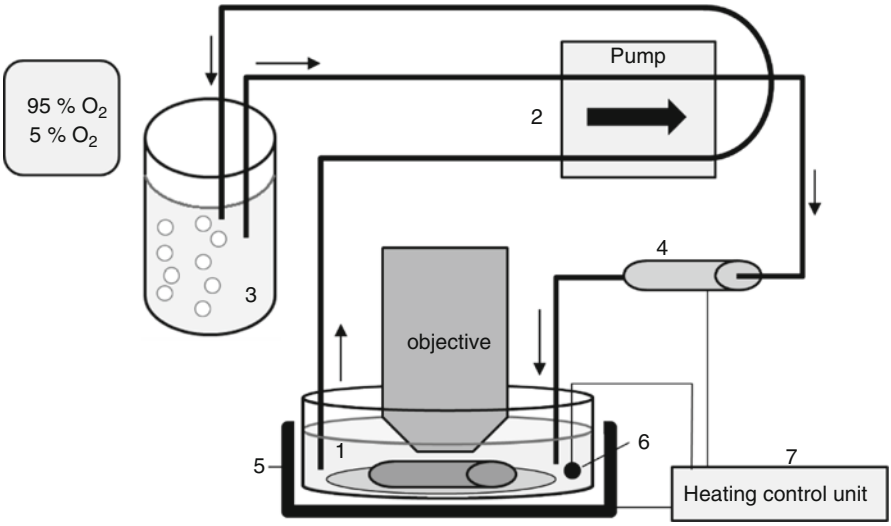

Fig. 7.3 Schematic diagram of recirculating superfusion and heating system to maintain aorta under physiological conditions during imaging. An aorta explant is incubated with T cells for 12 h to allow the T cells to migrate into the tissue. The artery is glued to a coverslip, and placed in a dish with complete RPMI 1,640 without phenol red, with 2 mM L-glutamine, 1 % pen/strep, and 1 % FBS. (*1*) A peristaltic pump (*2*) circulates the media from an oxygenated reservoir, (*3*) through an in-line solution heater (*4*), to the dish and back to the reservoir. The sample is warmed by a dish-warmer (*5*). The media temperature is monitored by a thermometer (*6*), and a control unit (*7*) regulates both heaters to maintain a solution temperature of 37 °C. *Arrows* show the direction of fluid flow

control unit (Warner Instruments, TC-334B) that maintained the liquid near the tissue at 37 °C. The peristaltic pump also returned the media from the dish to the reservoir so that the media constantly recirculate. The inlet and outlet to the dish must be as far as possible from the tissue to not disturb the imaging.

7.2.4 Microscopy and Hardware

Imaging was performed on a Leica TCS SP5 multiphoton system. This system utilizes a DM 6000 upright microscope with a 20× (NA = 0.95) water-dipping objective (Olympus, XLUMPLFL), attached to a piezo-controlled objective holder (Piezosystem Jena, NV 40/1 CLE and MIPOS 500 SG) to set the focal plane. A Coherent Chameleon Ultra II Ti:sapphire-pulsed femtosecond laser excites the sample with wavelengths between 680 nm and 1,080 nm. Emitted light is split through a series of three dichroic mirrors and four filters up to four non-descanned photomultiplier tube detectors (PMT-NDD) (Fig. 7.4). The optical path to the detectors does not return through the scanning mirror, improving the sensitivity of detection. Laser scanning is accomplished with either a conventional or resonant scanner, depending on the needs of the experiment. The resonant scanner scans each line faster than the conventional scanner

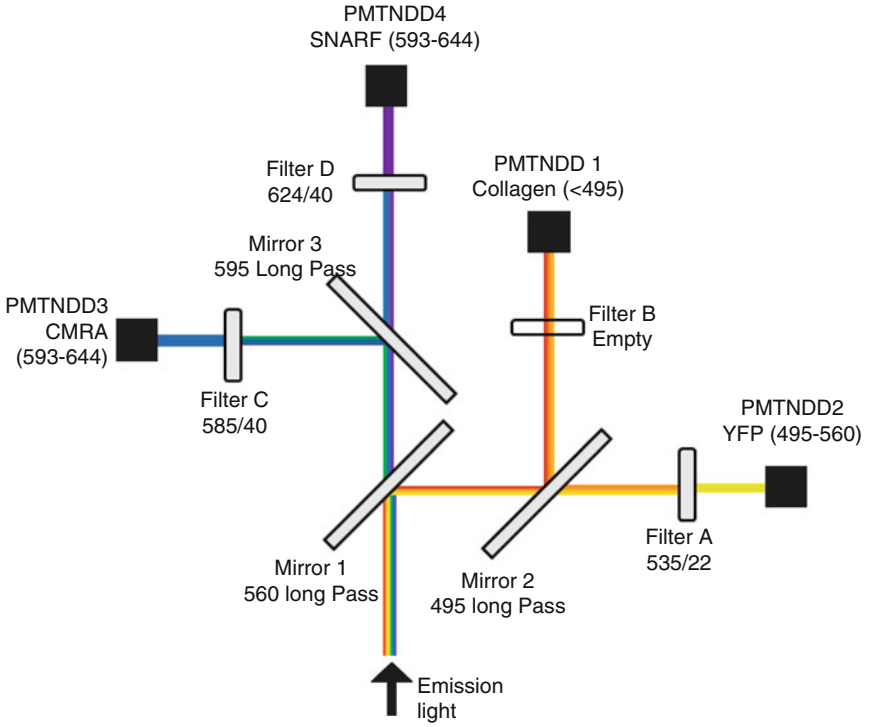

Fig. 7.4 Optical path with dichroic mirrors and filters to simultaneously detect emitted light from an aorta with YFP+ myeloid cells, CMRA-labeled T cells, and SNARF-labeled T cells as well as collagen via SHG. All dichroic mirrors are long-pass, and all filters are band-pass (width/middle). Each PMT is labeled with the fluorophore detected and the approximate wavelength range that reaches the detector

(8,000 lines/s compared to 200–1,400 lines/s). The speed can be effectively doubled in the bidirectional mode which allows for horizontal scanning in both directions, though this can lead to interlacing errors. The pixel dwell time of the resonant mode is shorter, which leads to a higher frame rate and less photobleaching, but more noise. Line or frame averaging can reduce this noise and may still allow for better time resolution than with a conventional scanner.

To observe interactions between YFP^+ antigen-presenting cells and SNARF- or CMRA-labeled T cells, the excitation laser was set to 920 nm. This wavelength allows for imaging of all three colors as well as collagen in the arterial wall via second-harmonic generation. The emitted light was split by three long-pass dichroic mirrors (495, 560, and 593 nm) into four bands and passed through three band-pass filters (535/22, 585/40, and 624/40 nm) (Semrock) (Fig. 7.4, Table 7.3). A large field of view (pixel size of ~1 μm) was chosen to capture as many cells as possible, although this does not allow for maximum spatial resolution as calculated by the Nyquist sampling frequency. The Nyquist frequency, which is the pixel size necessary to capture two points that are just optically resolved, is approximately 120 nm for two-photon excitation under our imaging conditions. Due to the inherent low axial resolution of two-photon excitation, 10–15 μm between z-planes was

Table 7.3 Typical hardware settings on Leica TCS SP5 multiphoton system with conventional scanner for imaging YFP + APCs, SNARF-labeled T cells, and CMRA-labeled T cells. See Fig. 7.4 for mirror and filter name explanations

Settings	Value	Comments
Dichroic 1	560 nm long pass	Optimized for simultaneous detection of YFP, SNARF, CMRA, and second-harmonic signal. Must be changed for any other color combination
Dichroic 2	495 nm long pass	
Dichroic 3	593 nm long pass	
Filter A	535/22	Detects YFP
Filter B	None	Detects second harmonic – no filter needed
Filter C	585/40	Detects CMRA
Filter D	624/40	Detects SNARF
PMT voltage	1,000–1,250 V	Set each PMT gain to almost the maximum and minimize laser power to reduce photobleaching
PMT offset	−10–0 %	Set such that tissue background is at or near 0
Excitation wavelength	900–920 nm	Optimized for combination of YFP, SNARF, and CMRA
Emitted laser power	2,200 mW	Determined by wavelength
Excitation neutral density filter	3 % [97 % blocked]	Highly dependent on individual laser and alignment. Blocking more reduces photobleaching
Laser gain	90–100 %	Keep as low as possible while detecting signal
Laser offset	50–60 %	Set such that there is no signal at 0 % laser gain
Frame size (pixels)	512×512	Higher for better spatial resolution, lower for faster scan speed and less photobleaching
Zoom	1×–2×	Zoom is a balance between improving spatial resolution by decreasing pixel size and increasing frame size to image more cells
Frame length (μm)	375–750 μm	
Pixel size (nm)	730–1,460 nm	
Scan speed	400 lines/s	Higher for faster frame rate, lower for less noise
Scan direction	1	Bidirectional scanning raises scan speed, but can lead to interlacing artifacts
Line/frame averaging	None	Averaging improves picture quality, but reduces frame rate and increases photobleaching
z-step	10–15 μm	Lower for better axial resolution but more photobleaching
Number of z-steps	8–20	From the adventitia to the deepest T cell
Stack frequency	1/min	Faster scan rates lead to more photobleaching and shorter movies, but better time resolution
Output format	LIF	Can be read by Imaris and ImageJ, or converted to TIF

sufficient for capturing cell location and shape while minimizing photobleaching. A full stack of 10–20 *z*-planes was acquired once per minute. Most of the exogenously added T cells were located in the adventitia, so typically only the outer layer of the artery was imaged. Taking advantage of the motorized stage, two to three locations were imaged concurrently by moving the sample between stacks. Aortas were imaged for roughly an hour, at which photobleaching became noticeable (Table 7.3).

These experimental settings were optimized for imaging with the conventional scanner. The spatial or temporal resolution of the movies could be improved with the resonant scanner by acquiring more *z*-planes or by acquiring stacks faster without a significant increase in photobleaching.

7.2.5 Image Processing

Autofluorescence signal was extracted from low-intensity pixels from YFP, CMRA, or SNARF channels, which were then combined and converted to a new channel. Autofluorescence comes mainly from the elastic lamina in the media layer [30] and can be used to distinguish the adventitia and intima. Collagen, visible through second-harmonic generation, is found in both the adventitia and media. Cell motion was quantified in three dimensions using an automated spot-tracking algorithm in Imaris (Bitplane) with occasional manual correction. The software detects cells based on difference in pixel intensity compared to background and then calculates the centroid of the cell. The cell centers are automatically tracked between frames using an auto-regressive motion algorithm, which assumes mostly random motion that tends towards the velocity and direction calculated in the previous frame. Dendritic projections of myeloid cells are often too thin (width <1 μm) or dim to be detected, so contact between T cells and APCs could not always be directly visualized. T cells were manually determined to be interacting with an APC when the T cell remained in the vicinity of a YFP+ cell for at least 5 min. Interaction times often ranged from 5 min to 1 h. Instantaneous velocity was calculated for each tracked cell between each pair of adjacent frames. Average velocity was calculated for interacting and noninteracting cells separately. Cells which did not move during the entire movie were presumed to be dead and not included in the statistics.

7.3 Results

Ex vivo multiphoton imaging of an explanted aorta allows for the visualization of live, active lymphocytes and myeloid cells within the intima and adventitia of the arterial wall. Collagen and elastin autofluorescence separates the intima from the adventitia. YFP+ myeloid cells were found in both the adventitia and intimal plaque of the aorta of atherosclerotic mice (Fig. 7.5). These cells move at approximately 1–3 μm/min, with significant deformation in cell shape as they travel.

Exogenously added T cells were typically only seen in the adventitial layer, although they can be found in intimal plaques when the plaque was exposed to the cells during the overnight incubation. These T cells migrate through the tissue at typical speeds of 10 μm/min (range 1–30 μm/min). When cognate antigen

Fig. 7.5 (**a**) Three different views of an aorta from an *Apoe*$^{-/-}$ *CD11cYFP* mouse fed WD to show localization of YFP+ cells to the intimal plaque and adventitia. *Green*, YFP+ cells; *Red*, SHG; *Blue*, autofluorescence from the internal elastic lamina (Adapted from Andor Technology [15]). (**b**) Cartoon depicting the anatomy of the aorta seen in (**a**)

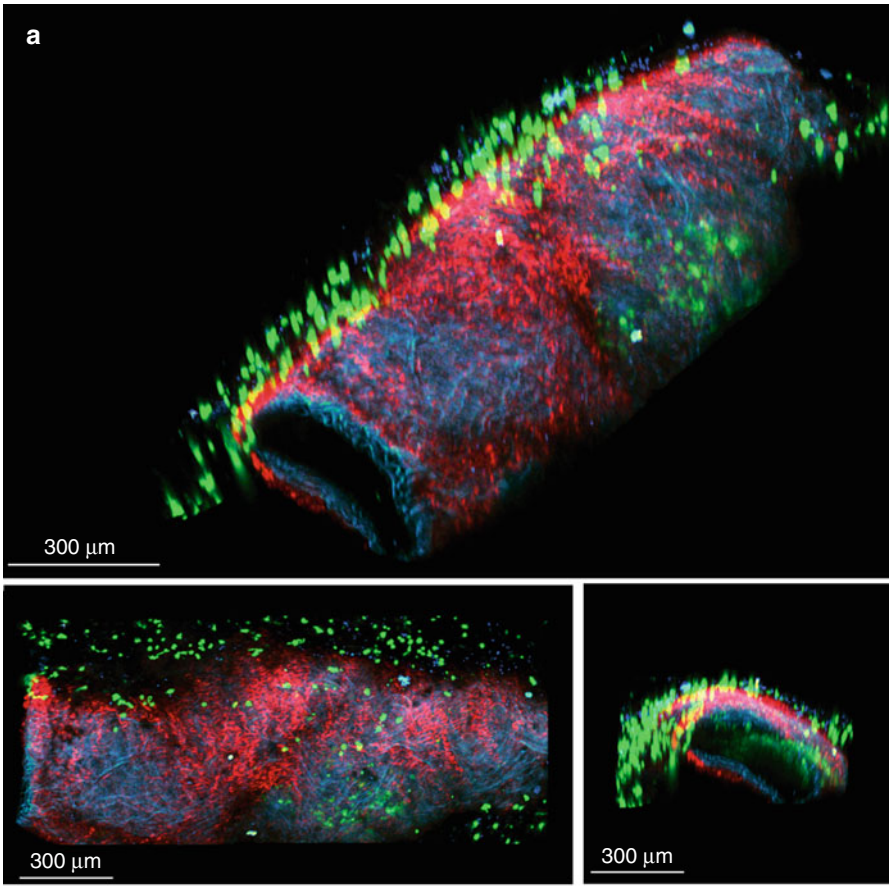
a
300 µm
300 µm
300 µm

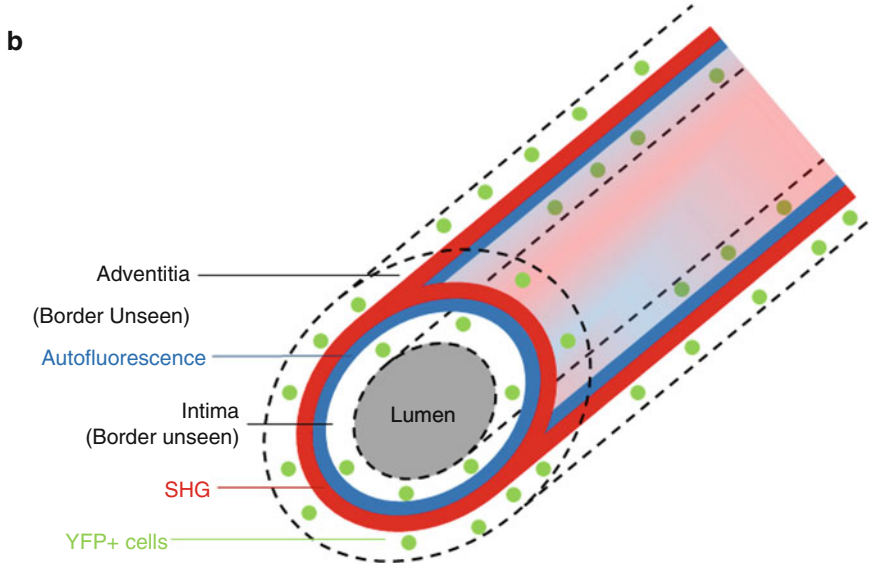
b
Adventitia
(Border Unseen)
Autofluorescence
Intima
(Border unseen)
SHG
YFP+ cells
Lumen

(exogenous or endogenous) is present, more T cells interact with YFP+ APCs, and the average velocity of the T cells decreases to 1–3 μm/s [9], suggesting antigen presentation is occurring within the arterial wall.

7.4 Conclusion and Future Work

This novel approach provides new opportunities to study cell activity that cannot be investigated with traditional static methods. This protocol could be expanded to the study of other questions relevant to disease pathology through the use of other transgenic reporter mice with a variety of fluorescently labeled cells or proteins. For instance, imaging cell migration can reveal novel information about chemokine function or the mechanism of how leukocytes enter and leave the aortic wall. Currently, ex vivo multiphoton imaging is the most suitable tool for probing these dynamic processes in their native environment to elucidate inflammatory mechanisms in atherosclerosis.

However, explanted tissue cannot completely mimic the native microenvironment that the leukocytes experience in vivo. Specifically, the absence of pulsatile blood flow [31], the disruption of the extracellular matrix in the adventitia [32, 33], and the alteration of oxygen concentration [34] or other changes from physiological conditions can influence cell motion [8]. Certain questions can only be accurately studied by imaging live mice, such as recruitment of monocytes from the blood to the plaque. New technical challenges are introduced when imaging leukocytes in arteries in vivo, because the blood vessel pulses with each heartbeat. This motion leads to distortion of still images, misalignment of z-stacks, and inconsistency in time series. These artifacts make tracking cells infeasible.

To circumvent these problems, we are currently developing a new technique that will minimize these motion artifacts and enable imaging of the carotid artery in vivo. Custom circuitry will trigger image acquisition based on the cardiac cycle, measured noninvasively through pulse oximetry. This ensures that the artery is in a consistent position for each frame acquired, so that z-stacks and time series can be reassembled accurately. Imaging only a small field of view with a fast acquisition speed after each trigger helps minimize in-frame deformation. These small sections can be stitched together in post-processing to assemble a large three-dimensional reconstruction of the cells in the artery. This system will enable us to image atherosclerotic plaques in vivo and to study various questions involving cell motility, including leukocyte recruitment from blood, antigen presentation, phagocytosis, chemokine function, and the role of cell subsets in disease progression.

References

1. World Health Organization. Global burden of disease, http://www.who.int/healthinfo/global_burden_disease/estimates_country/en/index.html (2013). Accessed 7 May 2013.

2. Galkina E, Ley K. Immune and inflammatory mechanisms of atherosclerosis. Annu Rev Immunol. 2009;27:165–97. doi:10.1146/annurev.immunol.021908.132620.
3. Galkina E, Kadl A, Sanders J, Varughese D, Sarembock IJ, Ley K. Lymphocyte recruitment into the aortic wall before and during development of atherosclerosis is partially L-selectin dependent. The Journal of experimental medicine. 2006;203(5):1273–82. doi:10.1084/jem.20052205.
4. Schulte S, Sukhova GK, Libby P. Genetically programmed biases in Th1 and Th2 immune responses modulate atherogenesis. Am J Pathol. 2008;172(6):1500–8. doi:10.2353/ajpath.2008.070776.
5. Egen JG, Rothfuchs AG, Feng CG, Horwitz MA, Sher A, Germain RN. Intravital imaging reveals limited antigen presentation and T cell effector function in mycobacterial granulomas. Immunity. 2011;34(5):807–19. doi:10.1016/j.immuni.2011.03.022.
6. Han JW, Shimada K, Ma-Krupa W, Johnson TL, Nerem RM, Goronzy JJ, Weyand CM. Vessel wall-embedded dendritic cells induce T-cell autoreactivity and initiate vascular inflammation. Circ Res. 2008;102(5):546–53. doi:10.1161/CIRCRESAHA.107.161653.
7. Choi JH, Do Y, Cheong C, Koh H, Boscardin SB, Oh YS, Bozzacco L, Trumpfheller C, Park CG, Steinman RM. Identification of antigen-presenting dendritic cells in mouse aorta and cardiac valves. J Exp Med. 2009;206(3):497–505. doi:10.1084/jem.20082129.
8. Miller MJ, Wei SH, Parker I, Cahalan MD. Two-photon imaging of lymphocyte motility and antigen response in intact lymph node. Science. 2002;296(5574):1869–73. doi:10.1126/science.1070051.
9. Mempel TR, Henrickson SE, Von Andrian UH. T-cell priming by dendritic cells in lymph nodes occurs in three distinct phases. Nature. 2004;427(6970):154–9. doi:10.1038/nature02238.
10. Koltsova EK, Garcia Z, Chodaczek G, Landau M, McArdle S, Scott SR, von Vietinghoff S, Galkina E, Miller YI, Acton ST, Ley K. Dynamic T cell-APC interactions sustain chronic inflammation in atherosclerosis. J Clin Invest. 2012;122(9):3114–26. doi:10.1172/JCI61758.
11. Frigault MM, Lacoste J, Swift JL, Brown CM. Live-cell microscopy - tips and tools. J Cell Sci. 2009;122(Pt 6):753–67. doi:10.1242/jcs.033837.
12. Stephens DJ, Allan VJ. Light microscopy techniques for live cell imaging. Science. 2003;300(5616):82–6. doi:10.1126/science.1082160.
13. Nikon. MicroscopyU-introduction to live-cell imaging techniques. http://www.microscopyu.com/articles/livecellimaging/index.html (2013). Accessed 26 Apr 2013.
14. Zeiss. Live-cell imaging. http://zeiss-campus.magnet.fsu.edu/articles/livecellimaging/index.html (2013). Accessed 26 Apr 2013.
15. Andor Technology. iXon Ultra 897. http://www.andor.com/pdfs/specifications/Andor_iXon_Ultra_897_Specifications.pdf (2013). Accessed 3 May 2013.
16. McNally JG, Karpova T, Cooper J, Conchello JA. Three-dimensional imaging by deconvolution microscopy. Methods. 1999;19(3):373–85. doi:10.1006/meth.1999.0873.
17. Leica. Leica SD AF – the integrated confocal spinning disk solution. http://www.leica-microsystems.com/news-media/news/news-details/article/leica-sd-af-the-integrated-confocalspinning-disk-solution/.
18. Ntziachristos V. Going deeper than microscopy: the optical imaging frontier in biology. Nat Methods. 2010;7(8):603–14. doi:10.1038/nmeth.1483.
19. Zipfel WR, Williams RM, Webb WW. Nonlinear magic: multiphoton microscopy in the biosciences. Nat Biotechnol. 2003;21(11):1369–77. doi:10.1038/nbt899.
20. Drobizhev M, Makarov NS, Tillo SE, Hughes TE, Rebane A. Two-photon absorption properties of fluorescent proteins. Nat Methods. 2011;8(5):393–9. doi:10.1038/nmeth.1596.
21. Taatjes DJ, Wadsworth MP, Schneider DJ, Sobel BE. Improved quantitative characterization of atherosclerotic plaque composition with immunohistochemistry, confocal fluorescence microscopy, and computer-assisted image analysis. Histochem Cell Biol. 2000;113(3):161–73.
22. Zoumi A, Yeh A, Tromberg BJ. Imaging cells and extracellular matrix in vivo by using second-harmonic generation and two-photon excited fluorescence. Proc Natl Acad Sci USA. 2002;99(17):11014–9. doi:10.1073/pnas.172368799.

23. Zhang SH, Reddick RL, Piedrahita JA, Maeda N. Spontaneous hypercholesterolemia and arterial lesions in mice lacking apolipoprotein E. Science. 1992;258(5081):468–47.
24. Lindquist RL, Shakhar G, Dudziak D, Wardemann H, Eisenreich T, Dustin ML, Nussenzweig MC. Visualizing dendritic cell networks in vivo. Nat Immunol. 2004;5(12):1243–50. doi:10.1038/ni1139.
25. Barnden MJ, Allison J, Heath WR, Carbone FR. Defective TCR expression in transgenic mice constructed using cDNA-based alpha- and beta-chain genes under the control of heterologous regulatory elements. Immunol Cell Biol. 1998;76(1):34–40. doi:10.1046/j.1440-1711.1998.00709.x.
26. Oxenius A, Bachmann MF, Zinkernagel RM, Hengartner H. Virus-specific MHC-class II-restricted TCR-transgenic mice: effects on humoral and cellular immune responses after viral infection. Eur J Immunol. 1998;28(1):390–400.
27. Hermansson A, Ketelhuth DF, Strodthoff D, Wurm M, Hansson EM, Nicoletti A, Paulsson-Berne G, Hansson GK. Inhibition of T cell response to native low-density lipoprotein reduces atherosclerosis. J Exp Med. 2010;207(5):1081–93. doi:10.1084/jem.20092243.
28. Palinski W, Horkko S, Miller E, Steinbrecher UP, Powell HC, Curtiss LK, Witztum JL. Cloning of monoclonal autoantibodies to epitopes of oxidized lipoproteins from apolipoprotein E-deficient mice. Demonstration of epitopes of oxidized low density lipoprotein in human plasma. J Clin Invest. 1996;98(3):800–14. doi:10.1172/JCI118853.
29. Schett G, Xu Q, Amberger A, Van der Zee R, Recheis H, Willeit J, Wick G. Autoantibodies against heat shock protein 60 mediate endothelial cytotoxicity. J Clin Invest. 1995;96(6):2569–77. doi:10.1172/JCI118320.
30. Zoumi A, Lu X, Kassab GS, Tromberg BJ. Imaging coronary artery microstructure using second-harmonic and two-photon fluorescence microscopy. Biophys J. 2004;87(4):2778–86. doi:10.1529/biophysj.104.042887.
31. Cinamon G, Shinder V, Alon R. Shear forces promote lymphocyte migration across vascular endothelium bearing apical chemokines. Nat Immunol. 2001;2(6):515–22. doi:10.1038/88710.
32. Megens RT, Reitsma S, Schiffers PH, Hilgers RH, De Mey JG, Slaaf DW, oude Egbrink MG, van Zandvoort MA. Two-photon microscopy of vital murine elastic and muscular arteries. Combined structural and functional imaging with subcellular resolution. J Vasc Res. 2007;44(2):87–98. doi:10.1159/000098259.
33. Sorokin L. The impact of the extracellular matrix on inflammation. Nat Rev Immunol. 2010;10(10):712–23. doi:10.1038/nri2852.
34. Caldwell CC, Kojima H, Lukashev D, Armstrong J, Farber M, Apasov SG, Sitkovsky MV. Differential effects of physiologically relevant hypoxic conditions on T lymphocyte development and effector functions. J Immunol. 2001;167(11):6140–9.